Geochronology, 5, 285–299, 2023
https://doi.org/10.5194/gchron-5-285-2023


# Amino acid racemization in *Neogloboquadrina pachyderma* and *Cibicidoides wuellerstorfi* from the Arctic Ocean and its implications for age models

**Gabriel West**[1,2], **Darrell S. Kaufman**[3], **Martin Jakobsson**[1,2], **and Matt O'Regan**[1,2]

[1]Department of Geological Sciences, Stockholm University, Stockholm, 10691, Sweden
[2]Bolin Centre for Climate Research, Stockholm University, Stockholm, 10691, Sweden
[3]School of Earth and Sustainability, Northern Arizona University, Flagstaff, AZ 86011, USA

**Correspondence:** Gabriel West (gabriel.west@geo.su.se) and Matt O'Regan (matt.oregan@geo.su.se)

Received: 3 October 2022 – Discussion started: 18 October 2022
Revised: 14 April 2023 – Accepted: 11 May 2023 – Published: 19 June 2023

**Abstract.** We report the results of amino acid racemization (AAR) analyses of aspartic acid (Asp) and glutamic acid (Glu) in the planktic *Neogloboquadrina pachyderma*, and the benthic *Cibicidoides wuellerstorfi*, foraminifera species collected from sediment cores from the Arctic Ocean. The cores were retrieved at various deep-sea sites of the Arctic, which cover a large geographical area from the Greenland and Iceland seas (GIS) to the Alpha and Lomonosov ridges in the central Arctic Ocean. Age models for the investigated sediments were developed by multiple dating and correlation techniques, including oxygen isotope stratigraphy, magnetostratigraphy, biostratigraphy, lithostratigraphy, and cyclostratigraphy. The extent of racemization (D/L values) was determined on 95 samples (1028 subsamples) and shows a progressive increase downcore for both foraminifera species. Differences in the rates of racemization between the species were established by analysing specimens of both species from the same stratigraphic levels ($n = 21$). Aspartic acid (Asp) and glutamic acid (Glu) racemize on average $16 \pm 2$ % and $23 \pm 3$ % faster, respectively, in *C. wuellerstorfi* than in *N. pachyderma*. The D/L values increase with sample age in nearly all cases, with a trend that follows a simple power function. Scatter around least-squares regression fits are larger for samples from the central Arctic Ocean than for those from the Nordic Seas. Calibrating the rate of racemization in *C. wuellerstorfi* using independently dated samples from the Greenland and Iceland seas for the past 400 ka enables estimation of sample ages from the central Arctic Ocean, where bottom water temperatures are presently relatively similar. The resulting ages are older than expected when considering the existing age models for the central Arctic Ocean cores. These results confirm that the differences are not due to taxonomic effects on AAR and further warrant a critical evaluation of existing Arctic Ocean age models. A better understanding of temperature histories at the investigated sites, and other environmental factors that may influence racemization rates in central Arctic Ocean sediments, is also needed.

## 1 Introduction

The first application of amino acid geochronology to Arctic Ocean sediments analysed the extent of epimerization in the protein amino acid, isoleucine, over time in samples of the planktic, *Neogloboquadrina pachyderma*, and the benthic, *Cibicidoides wuellerstorfi*, foraminifera species (Sejrup et al., 1984). Not only did this study provide some of the first amino acid racemization (AAR) data from a polar environment, but it also exposed crucial chronological issues associated with Arctic Ocean sediments. The results contradicted available age interpretations obtained from palaeomagnetic data (Sejrup et al., 1984; Backman et al., 2004). The problems of dating Pleistocene Arctic marine sediments continue to exist today and are well known (e.g. Alexanderson et al., 2014). Over the past few decades, amino acid geochronology received limited attention in the Arctic, but several studies provided promising results (Sejrup and Haugen, 1992; Kauf-

man et al., 2008, 2013) that highlighted its potential as a dating technique and the need for its continued development in Arctic settings. This is particularly desirable, since theoretically, it could provide age control up to a few million years, using even limited amounts of calcium carbonate.

*N. pachyderma* and *C. wuellerstorfi* are commonly used in stable isotope stratigraphy and palaeoceanographic reconstructions (e.g. Shackleton et al., 2003) and are associated with cold water masses. *N. pachyderma* is considered to be a primarily "high-latitude" species (Darling et al., 2017), and *C. wuellerstorfi* is thought to show strong preference for bottom waters below ∼ 5 °C (Rasmussen and Thomsen, 2017). These characteristics and their frequent occurrence in sediment cores from the Arctic Ocean make them particularly useful for amino acid geochronology studies in this region.

The rates of racemization for aspartic acid (Asp) and glutamic acid (Glu) were previously calibrated in *N. pachyderma* from central Arctic Ocean samples by Kaufman et al. (2008) for the past 150 ka. The calibration relied on the established age models of sediments from the Lomonosov Ridge (O'Regan et al., 2008). Subsequently, however, the extent of racemization in these samples was shown to be higher than expected when compared with those of similar ages from other cold bottom water sites from the Atlantic and Pacific oceans (Kaufman et al., 2013), despite the cold bottom water in the central Arctic Ocean. The reason for this apparently higher extent of racemization in *N. pachyderma* from central Arctic Ocean samples is unclear, but not considered to be caused by taxonomic effects, since the rate of racemization observed in this species is lower than in other taxa (Kaufman et al., 2013). Either the established ages that were used to calibrate the rate of racemization in the central Arctic Ocean sediments are too young, such that units currently correlated with substages of marine oxygen isotope stage (MIS) 5 instead represent MIS 9, 7, and 5, or other undetermined processes influence protein degradation and preservation in central Arctic Ocean foraminifera. At the Yermak Plateau in the eastern Arctic Ocean (Fig. 1), racemization rates for *N. pachyderma* generally conform to the rates determined for other cold bottom water sites (West et al., 2019), further challenging the established ages previously used to calibrate the rate of AAR from the Lomonosov Ridge in the central Arctic Ocean. However, it is unknown how racemization progresses in other regions of the Arctic Ocean.

If the apparently higher extent of racemization in *N. pachyderma* from the central Arctic Ocean is not the result of taxonomic effects, a higher rate of racemization can also be anticipated in other taxa from the area, e.g. in *C. wuellerstorfi*. However, little is known about racemization of amino acids in this species. The earliest studies involving *C. wuellerstorfi* investigated taxonomical applications (Haugen et al., 1989) or focused on the epimerization of isoleucine (Sejrup et al., 1984; Sejrup and Haugen, 1992) utilizing high-performance liquid chromatograph (HPLC) ion exchange analysers. Since the publication of these seminal papers, analysis of amino acids has become significantly faster, with reduced sample mass requirements, due to improvements in analytical methods (Kaufman and Manley, 1998), yet no studies have addressed amino acid racemization in *C. wuellerstorfi* despite its palaeoceanographical importance (e.g. Yu and Elderfield, 2008; Wollenburg et al., 2015; Burkett et al., 2016; Raitzsch et al., 2020) and the relatively faster and easier sample processing offered by its larger tests (up to ∼ 4–5 times the size) when compared to *N. pachyderma*.

Here, we report the results of aspartic acid and glutamic acid racemization analyses of *N. pachyderma* and *C. wuellerstorfi* obtained from well-dated Quaternary deep-sea sediment cores from the Greenland and Iceland seas (GIS), and from sediment cores from the central Arctic Ocean, where sediment ages continue to be debated (Purcell et al., 2022). The long-term rates of racemization in the two species are compared, and the relationship between the extent of racemization and sample age is investigated in both species.

## 2 Materials and methods

### 2.1 Investigated sediment cores

Foraminifera samples were taken from sediment cores from the Greenland and Iceland seas, the Lomonosov Ridge, and the Alpha Ridge (Fig. 1). The Greenland and Iceland seas, although part of the Arctic Ocean, are under the direct influence of Atlantic surface waters, and thus are predominantly characterized by open water conditions, unlike the sea-ice-covered areas of the Lomonosov and Alpha ridges. The studied sediment cores (Table 1) were collected from deep-water (811–2952 m) environments, which presently experience similar, very cold ($< 0$ °C), and relatively stable bottom water temperatures.

Age–depth models for the investigated sediment cores have been developed using a variety of dating techniques. Cores from the Nordic Seas (ODP151/907A and PS17/1906-2) primarily relied on oxygen isotope stratigraphy, complemented by magnetostratigraphy in the case of ODP151/907A (Jansen et al., 2000a, b), and by carbon isotope stratigraphy for core PS17/1906-2 (Bauch, 2002, 2013). The age–depth model of the latter is less certain beyond the marine isotope stage (MIS) 6 (Bauch, 2013) due to the large uncertainty associated with isotope stratigraphy, a characteristic issue of Arctic Ocean records.

The age–depth models of sediment cores from the central Arctic Ocean utilize a more diverse toolset, reflecting the difficulties of dating Arctic marine sediments, and heavily depend on a combination of bio- and lithostratigraphy (e.g. Cronin et al., 2019). The lithostratigraphy of the central Arctic Ocean cores investigated in this study can be correlated with that of the Integrated Ocean Drilling Program (IODP) Expedition 302, the Arctic Coring Expedition (ACEX). This correlation is most apparent in bulk density

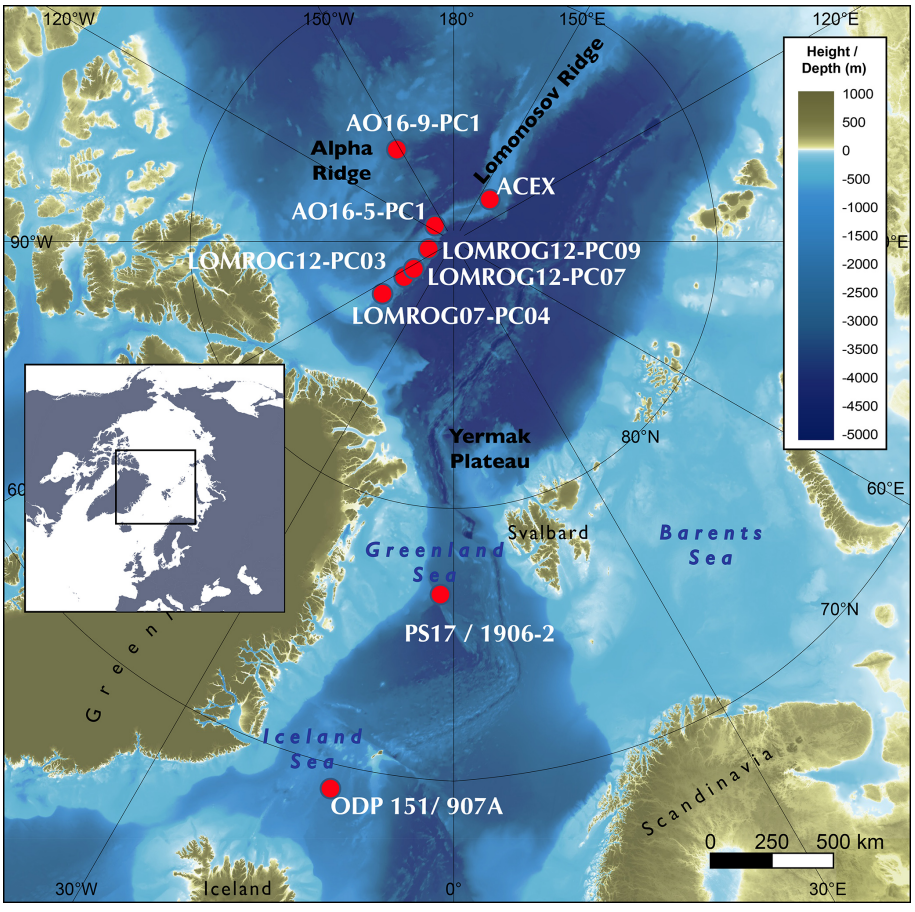


**Figure 1.** Location of sediment cores referred to in this study. Basemap: Jakobsson et al. (2020).

**Table 1.** Sediment cores investigated in this study. Current bottom water temperatures were approximated by using annual mean temperature observations from the nearest location from the World Ocean Atlas (Locarnini et al., 2018).

| Region | Core | Latitude (°) | Longitude (°) | Water depth (m) | Bottom water temperature est. (°C) | Age reference |
|---|---|---|---|---|---|---|
| Alpha Ridge | AO16-9-PC1 | 85.95570 | −148.32580 | 2212 | −0.4 | Cronin et al. (2019) |
| Lomonosov Ridge | AO16-5-PC1 | 89.07800 | −130.54700 | 1253 | −0.3 | ACEX age model* |
| Lomonosov Ridge | LOMROG07-PC04 | 86.70117 | −53.76720 | 811 | 0.1 | Hanslik et al. (2013) |
| Lomonosov Ridge | LOMROG12-PC03 | 87.72470 | −54.42528 | 1607 | −0.4 | O'Regan et al. (2020) |
| Lomonosov Ridge | LOMROG12-PC07 | 88.19760 | −55.68450 | 2952 | −0.8 | ACEX age model* |
| Lomonosov Ridge | LOMROG12-PC09 | 89.02672 | −73.73444 | 1318 | −0.3 | ACEX age model* |
| Iceland Sea | ODP 151/907A | 69.24982 | 12.69823 | 1801 | −0.8 | Jansen et al. (2000a, b) |
| Greenland Sea | PS17/1906-2 | 76.84630 | −2.15050 | 2901 | −1.0 | Bauch (2002, 2013) |

* The ACEX age model is based on Backman et al. (2008), Frank et al. (2008), and O'Regan et al. (2008).

profiles (Fig. 2), but other sedimentological properties including grain size and a variety of X-ray fluorescence (XRF) scanning properties also correlate coherently among cores (O'Regan et al., 2019). The currently accepted age model for the ACEX sedimentary sequence was developed using cyclostratigraphic analysis (O'Regan et al., 2008) and produced similar estimated Quaternary sedimentation rates as obtained by the decay of beryllium isotopes (Frank et al., 2008). The late Quaternary chronology (MIS 1–6) for ACEX included constraints from $^{14}$C dating and the correlation with nearby records AO96/12-1PC (Jakobsson et al., 2001) and PS2185 (Spielhagen et al., 2004), where MIS 5 was iden-

tified based on the occurrence of the calcareous nannofossil *Emiliania huxleyi* (Jakobsson et al., 2001); it was further supported by results from optically stimulated luminescence dating of quartz grains (Jakobsson et al., 2003). The age model of core LOMROG07-PC04 is based on correlation with PS2185 (Hanslik et al., 2013).

### 2.2 Analytical procedures

Sediment samples were wet sieved (63 µm) and air dried prior to picking foraminifera tests of *N. pachyderma* and *C. wuellerstorfi*. Initially, the > 250 µm fraction was targeted to isolate the largest and best-preserved tests. This was not possible for some samples, and the tests were collected from the 180–250 µm fraction instead. The tests were kept in glass vials and stored in a refrigerator prior to racemization analyses. A total of 95 stratigraphic depths were sampled, with some depths containing both foraminifera species ($n = 21$). Each sample was further subsampled – on average with 9.6 *N. pachyderma* and 11.2 *C. wuellerstorfi* subsamples per sample, producing 1009 analysed subsamples. Each subsample comprised between 10 and 12 *N. pachyderma* or 2 and 4 *C. wuellerstorfi* tests.

The analytical procedures followed that of previous analyses as described in detail by Kaufman et al. (2013) and West et al. (2019), and they were performed at the Amino Acid Geochronology Laboratory (AAGL), Northern Arizona University. The foraminifera tests were first sonicated (1–30 s) to remove any loose sediment particles, treated with 1 mL hydrogen peroxide (3 %) to remove surficial organic matter, and then rinsed three times with reagent grade (grade I) water. Multiple tests were picked into micro-reaction hydrolysis vials (defining one subsample) and dissolved in 8 µL hydrochloric acid (6 M). The vials were then sealed with nitrogen gas and the subsamples hydrolysed for 6 h at 110 °C. After the hydrolysis was complete, the subsamples were evaporated in a vacuum desiccator and then rehydrated in 4 µL of 0.01 M HCl spiked with 10 µM L-*homo*arginine. Each subsample was injected onto a high-performance liquid chromatograph (HPLC) with a fully automated, reversed phase procedure (Kaufman and Manley, 1998) to separate pairs of D- and L-amino acids. The peak-area ratio of D/L stereoisomers of eight amino acids (aspartic acid, glutamic acid, serine (Ser), alanine, valine, phenylalanine, isoleucine, and leucine) were analysed to determine the extent of racemization. This study only utilized the racemization results of aspartic acid (Asp) and glutamic (Glu) acid, which are among the two most abundant and chronographically well-resolved amino acids. The Asp and Glu reported in this study also include any Asn and Gln present in the biomineral.

## 3 Results

### 3.1 Data screening

Initial data screening was based on the procedure of Kosnik and Kaufman (2008). First, subsamples with L-Ser/L-Asp $\geq 0.8$ – an indicator of potential contamination by modern amino acids – were excluded. The D/L values of Asp and Glu positively covary in fossil proteins. Subsamples that did not adhere to this expected trend were omitted. Finally, subsamples with D/L Asp or Glu values beyond $\pm 2\sigma$ of the sample mean were also removed (Fig. S1 in the Supplement). As a result of this screening process, 17.9 % of all subsamples were rejected (Table S1 in the Supplement).

Following the subsample screening process, sample means and related standard deviation values were calculated for Asp and Glu for all samples. Stratigraphically reversed samples (mean D/L values lower than expected for their stratigraphic depths with no overlap within $1\sigma$ with the sample from shallower depth) were identified within each core (Table 2). These include five samples of *N. pachyderma* and three of *C. wuellerstorfi*. Of these, two samples contained sufficient tests of both species to analyse AAR, but only *C. wuellerstorfi* were stratigraphically reversed.

### 3.2 Interspecies comparison

The overall subsample rejection rate was higher for *N. pachyderma* (22.7 %) than for *C. wuellerstorfi* (9.9 %) (Table 3). Only one *C. wuellerstorfi* subsample was rejected due to high serine content (L-Ser/L-Asp $\geq 0.8$), significantly fewer than those for *N. pachyderma*, implying that secondary amino acids (contamination) were not introduced during core storage or laboratory analysis because both species were treated similarly.

The proportion of samples with high intra-sample variability (coefficient of variation for D/L Asp and Glu > 10 %, following data screening) was approximately twice as high for *N. pachyderma* than for *C. wuellerstorfi*.

The rate of amino acid racemization varies between different foraminifera species (King and Neville, 1977). As some samples ($n = 21$) from certain stratigraphic intervals contained specimens of both *N. pachyderma* and *C. wuellerstorfi*, this allowed a direct comparison of the rates of racemization in the two species (Fig. 3). One stratigraphically reversed sample was omitted prior to analysis. The slope of the least-squares regression fit to the D/L versus D/L data indicates that Asp racemized, on average, $15 \pm 2$ % ($n = 19$) faster in *C. wuellerstorfi* than in *N. pachyderma*, and similarly, Glu also racemized faster ($23 \pm 2$ %) in *C. wuellerstorfi* than in *N. pachyderma*.

**Table 2.** Extent of racemization (D/L) for aspartic acid (Asp) and glutamic acid (Glu) in samples of *Neogloboquadrina pachyderma* and *Cibicidoides wuellerstorfi* from Arctic Ocean sediment cores. Reported ages are from published age models (Table 1).

| Lab ID (UAL) | Core | Core depth (m) | Age (ka) | $n$[a] | Excluded | Excl. ratio (%) | Asp D/L | 1$\sigma$ | Glu D/L | 1$\sigma$ |
|---|---|---|---|---|---|---|---|---|---|---|
| *Neogloboquadrina pachyderma* | | | | | | | | | | |
| | Alpha Ridge | | | | | | | | | |
| 17336 | AO16-9-PC1 | 0.190 | 16 | 10 | 1 | 10 | 0.141 | 0.014 | 0.069 | 0.011 |
| 17337 | AO16-9-PC1 | 0.210 | 22 | 10 | 1 | 10 | 0.210 | 0.010 | 0.104 | 0.005 |
| 17338 | AO16-9-PC1 | 0.970 | 127 | 8 | 3 | 38 | 0.419 | 0.020 | 0.242 | 0.029 |
| 17339 | AO16-9-PC1 | 1.260 | 188 | 10 | 5 | 50 | 0.445 | 0.015 | 0.254 | 0.022 |
| | Lomonosov Ridge | | | | | | | | | |
| 21406 | LOMROG12-TWC03 | 0.095 | 38 | 7 | 1 | 14 | 0.193 | 0.017 | 0.077 | 0.010 |
| 21407 | LOMROG12-TWC03 | 0.495 | 60 | 7 | 1 | 14 | 0.332 | 0.017 | 0.168 | 0.022 |
| 21408 | LOMROG12-PC03 | 0.505 | 61 | 8 | 2 | 25 | 0.340 | 0.032 | 0.163 | 0.026 |
| 21409 | LOMROG12-PC03 | 0.610 | 76 | 8 | 1 | 13 | 0.395 | 0.021 | 0.206 | 0.015 |
| 21410 | LOMROG12-PC03 | 0.761 | 108 | 8 | 3 | 38 | 0.415 | 0.040 | 0.212 | 0.025 |
| 21411 | LOMROG12-PC03 | 1.291 | 204 | 8 | 2 | 25 | 0.468 | 0.015 | 0.240 | 0.010 |
| 21412 | LOMROG12-PC03 | 1.401 | 236 | 6 | 2 | 33 | 0.443 | 0.021 | 0.239 | 0.026 |
| 21413 | LOMROG12-PC03 | 1.551 | 290 | 6 | 2 | 33 | 0.466 | 0.066 | 0.242 | 0.070 |
| 21414 | LOMROG12-PC03 | 1.601 | 311 | 8 | 3 | 38 | 0.417 | 0.032 | 0.185 | 0.026 |
| 21415 | LOMROG12-PC03 | 1.781 | 391 | 5 | 0 | 0 | 0.377 | 0.060 | 0.191 | 0.048 |
| 21416 | LOMROG12-PC03 | 2.101 | 489 | 8 | 5 | 63 | 0.392 | 0.037 | 0.207 | 0.040 |
| 22759 | LOMROG07-PC04 | 0.025 | MIS 1–3? (~ 19) | 17 | 4 | 24 | 0.102 | 0.018 | 0.044 | 0.011 |
| 21587 | LOMROG07-PC04 | 0.040 | MIS 1–3? (~ 39) | 8 | 3 | 38 | 0.097 | 0.006 | 0.036 | 0.004 |
| 21588 | LOMROG07-PC04 | 0.140 | MIS 5.1? (~ 77) | 8 | 3 | 38 | 0.278 | 0.034 | 0.114 | 0.021 |
| 22760 | LOMROG07-PC04 | 0.225 | MIS 5.1? (~ 82) | 11 | 1 | 9 | 0.278 | 0.008 | 0.123 | 0.009 |
| 22761 | LOMROG07-PC04 | 1.025 | MIS 5.5? (~ 115) | 13 | 2 | 15 | 0.320 | 0.011 | 0.151 | 0.012 |
| 21589 | LOMROG07-PC04 | 1.110 | MIS 5.5? (~ 123) | 8 | 4 | 50 | 0.347 | 0.029 | 0.146 | 0.022 |
| 22762 | LOMROG07-PC04 | 1.385 | > MIS 7? (~ 405) | 13 | 2 | 15 | 0.387 | 0.029 | 0.195 | 0.032 |
| [b]21590 | LOMROG07-PC04 | 1.410 | MIS 1–3? (~ 12.8) | 8 | 3 | 38 | 0.318 | 0.035 | 0.137 | 0.035 |
| 21591 | LOMROG07-PC04 | 1.720 | MIS 1–3? (~ 40) | 8 | 3 | 38 | 0.391 | 0.036 | 0.175 | 0.043 |
| 22763 | LOMROG07-PC04 | 1.785 | MIS 5.1? (~ 74) | 12 | 4 | 33 | 0.386 | 0.023 | 0.187 | 0.016 |
| 21592 | LOMROG07-PC04 | 2.010 | MIS 5.1? (~ 78) | 8 | 7 | 88 | 0.357 | | 0.140 | |
| 22764 | LOMROG07-PC04 | 2.025 | MIS 5.5? (~ 115) | 9 | 2 | 22 | 0.417 | 0.069 | 0.230 | 0.066 |
| [b]21594 | LOMROG07-PC04 | 3.000 | MIS 5.5? (~ 123) | 7 | 4 | 57 | 0.270 | 0.099 | 0.136 | 0.057 |
| 15866 | LOMROG12-PC07 | 0.020 | 9 | 9 | 2 | 22 | 0.081 | 0.004 | 0.034 | 0.002 |
| 15867 | LOMROG12-PC07 | 0.165 | 31 | 10 | 1 | 10 | 0.205 | 0.036 | 0.090 | 0.022 |
| 15868 | LOMROG12-PC07 | 0.315 | 40 | 10 | 2 | 20 | 0.272 | 0.025 | 0.124 | 0.013 |
| 15869 | LOMROG12-PC07 | 0.780 | 52 | 9 | 1 | 11 | 0.294 | 0.026 | 0.122 | 0.019 |
| 15870 | LOMROG12-PC07 | 0.980 | 63 | 6 | 1 | 17 | 0.354 | 0.024 | 0.163 | 0.022 |
| 15871 | LOMROG12-PC07 | 1.170 | 79 | 9 | 3 | 33 | 0.373 | 0.029 | 0.189 | 0.028 |
| 15872 | LOMROG12-PC07 | 1.425 | 96 | 9 | 3 | 33 | 0.399 | 0.035 | 0.183 | 0.027 |
| 15873 | LOMROG12-PC07 | 1.580 | 111 | 9 | 2 | 22 | 0.368 | 0.030 | 0.168 | 0.024 |
| 15874 | LOMROG12-PC07 | 1.720 | 124 | 9 | 3 | 33 | 0.385 | 0.024 | 0.173 | 0.025 |
| [b]15875 | LOMROG12-PC07 | 3.537 | 350 | 9 | 3 | 33 | 0.305 | 0.036 | 0.133 | 0.018 |
| 15876 | LOMROG12-PC07 | 3.657 | 374 | 9 | 0 | 0 | 0.354 | 0.048 | 0.185 | 0.031 |
| 15877 | LOMROG12-PC07 | 3.787 | 402 | 4 | 3 | 75 | 0.348 | | 0.174 | |
| 15878 | LOMROG12-PC07 | 4.210 | 485 | 6 | 3 | 50 | 0.402 | 0.012 | 0.193 | 0.011 |
| [b]15879 | LOMROG12-PC07 | 4.405 | 502 | 7 | 2 | 29 | 0.335 | 0.014 | 0.155 | 0.012 |
| 15880 | LOMROG12-PC07 | 4.510 | 510 | 5 | 3 | 60 | 0.307 | 0.029 | 0.145 | 0.034 |
| 22765 | LOMROG12-PC09 | 0.800 | 55 | 17 | 2 | 12 | 0.379 | 0.012 | 0.197 | 0.010 |
| 22766 | LOMROG12-PC09 | 1.250 | 129 | 10 | 0 | 0 | 0.400 | 0.029 | 0.209 | 0.030 |
| 22767 | LOMROG12-PC09 | 1.840 | 205 | 12 | 2 | 17 | 0.416 | 0.023 | 0.207 | 0.027 |
| 22768 | LOMROG12-PC09 | 1.980 | 233 | 17 | 3 | 18 | 0.435 | 0.019 | 0.232 | 0.024 |
| 22769 | LOMROG12-PC09 | 2.160 | 276 | 13 | 1 | 8 | 0.475 | 0.053 | 0.278 | 0.040 |
| [b]22770 | LOMROG12-PC09 | 3.400 | 603 | 11 | 4 | 36 | 0.407 | 0.005 | 0.203 | 0.006 |

**Table 2.** Continued.

| Lab ID (UAL) | Core | Core depth (m) | Age (ka) | $n$[a] | Excluded | Excl. ratio (%) | Asp D/L | 1$\sigma$ | Glu D/L | 1$\sigma$ |
|---|---|---|---|---|---|---|---|---|---|---|
| *Neogloboquadrina pachyderma* | | | | | | | | | | |
| | Iceland Sea | | | | | | | | | |
| 22745 | ODP 151/907A | 1.050 | 42 | 14 | 2 | 14 | 0.200 | 0.008 | 0.079 | 0.006 |
| 22746 | ODP 151/907A | 1.870 | 107 | 13 | 2 | 15 | 0.281 | 0.005 | 0.114 | 0.003 |
| 22747 | ODP 151/907A | 2.350 | 131 | 17 | 2 | 12 | 0.325 | 0.011 | 0.146 | 0.009 |
| 22748 | ODP 151/907A | 3.060 | 168 | 15 | 0 | 0 | 0.355 | 0.011 | 0.171 | 0.009 |
| 22749 | ODP 151/907A | 5.060 | 309 | 17 | 2 | 12 | 0.395 | 0.016 | 0.192 | 0.014 |
| 22750 | ODP 151/907A | 6.810 | 398 | 12 | 1 | 8 | 0.388 | 0.013 | 0.183 | 0.016 |
| 22751 | ODP 151/907A | 15.210 | 781 | 10 | 3 | 30 | 0.482 | 0.036 | 0.250 | 0.046 |
| | Greenland Sea | | | | | | | | | |
| 22732 | PS17/1906-2 | 0.150 | 10 | 12 | 3 | 25 | 0.129 | 0.003 | 0.067 | 0.004 |
| 22733 | PS17/1906-2 | 1.805 | 85 | 17 | 0 | 0 | 0.263 | 0.008 | 0.111 | 0.008 |
| 22734 | PS17/1906-2 | 2.005 | 111 | 12 | 0 | 0 | 0.306 | 0.006 | 0.138 | 0.005 |
| 22735 | PS17/1906-2 | 2.105 | 117 | 12 | 4 | 33 | 0.312 | 0.010 | 0.141 | 0.009 |
| 22736 | PS17/1906-2 | 2.205 | 122 | 12 | 3 | 25 | 0.347 | 0.011 | 0.169 | 0.012 |
| 22737 | PS17/1906-2 | 3.290 | 207 | 8 | 1 | 13 | 0.343 | 0.011 | 0.171 | 0.008 |
| 22738 | PS17/1906-2 | 3.605 | 225 | 12 | 2 | 17 | 0.355 | 0.010 | 0.178 | 0.010 |
| 22739 | PS17/1906-2 | 5.505 | 398 | 5 | 1 | 20 | 0.439 | 0.030 | 0.227 | 0.036 |
| *Cibicidoides wuellerstorfi* | | | | | | | | | | |
| | Alpha Ridge | | | | | | | | | |
| 17341 | AO16-9-PC1 | 0.190 | 16 | 10 | 0 | 0 | 0.235 | 0.061 | 0.099 | 0.040 |
| 17342 | AO16-9-PC1 | 0.210 | 22 | 10 | 1 | 10 | 0.326 | 0.027 | 0.158 | 0.020 |
| 17343 | AO16-9-PC1 | 0.970 | 127 | 10 | 0 | 0 | 0.502 | 0.005 | 0.311 | 0.010 |
| 17344 | AO16-9-PC1 | 1.260 | 188 | 10 | 0 | 0 | 0.522 | 0.007 | 0.321 | 0.008 |
| 17346 | AO16-9-PC1 | 2.415 | 599 | 10 | 2 | 20 | 0.523 | 0.101 | 0.302 | 0.094 |
| | Lomonosov Ridge | | | | | | | | | |
| 17331 | AO16-5-PC1 | 0.090 | 30 | 10 | 1 | 10 | 0.342 | 0.012 | 0.155 | 0.006 |
| 17333 | AO16-5-PC1 | 1.370 | 105 | 7 | 1 | 14 | 0.525 | 0.020 | 0.339 | 0.032 |
| 22752 | LOMROG12-TWC03 | 0.025 | 16 | 13 | 1 | 8 | 0.144 | 0.012 | 0.047 | 0.006 |
| 22753 | LOMROG12-TWC03 | 0.095 | 38 | 18 | 3 | 17 | 0.157 | 0.014 | 0.053 | 0.006 |
| 17327 | LOMROG12-TWC03 | 0.215 | 44 | 8 | 0 | 0 | 0.341 | 0.006 | 0.161 | 0.006 |
| 22754 | LOMROG12-PC03 | 0.520 | 66 | 13 | 3 | 23 | 0.412 | 0.014 | 0.208 | 0.013 |
| 17328 | LOMROG12-PC03 | 0.540 | 98 | 8 | 0 | 0 | 0.433 | 0.009 | 0.234 | 0.009 |
| 17329 | LOMROG12-PC03 | 0.741 | 198 | 8 | 1 | 13 | 0.485 | 0.008 | 0.284 | 0.008 |
| 17330 | LOMROG12-PC03 | 1.271 | 63 | 8 | 1 | 13 | 0.541 | 0.010 | 0.328 | 0.019 |
| [b]22755 | LOMROG12-PC03 | 1.441 | 247 | 9 | 1 | 11 | 0.491 | 0.017 | 0.267 | 0.035 |
| 22756 | LOMROG12-PC09 | 0.800 | 73 | 12 | 1 | 8 | 0.433 | 0.011 | 0.236 | 0.011 |
| 22757 | LOMROG12-PC09 | 1.250 | 140 | 22 | 2 | 9 | 0.476 | 0.007 | 0.266 | 0.011 |
| 22758 | LOMROG12-PC09 | 1.980 | 224 | 5 | 0 | 0 | 0.508 | 0.015 | 0.281 | 0.015 |
| | Iceland Sea | | | | | | | | | |
| 22740 | ODP 151/907A | 1.050 | 42 | 9 | 3 | 33 | 0.166 | 0.026 | 0.059 | 0.013 |
| 22741 | ODP 151/907A | 1.870 | 107 | 21 | 1 | 5 | 0.337 | 0.015 | 0.151 | 0.010 |
| [b]22742 | ODP 151/907A | 2.350 | 131 | 15 | 6 | 40 | 0.160 | 0.013 | 0.064 | 0.006 |
| 22743 | ODP 151/907A | 3.060 | 168 | 10 | 1 | 10 | 0.388 | 0.025 | 0.198 | 0.026 |
| 22744 | ODP 151/907A | 15.210 | 781 | 18 | 1 | 6 | 0.549 | 0.016 | 0.345 | 0.032 |
| | Greenland Sea | | | | | | | | | |
| 22724 | PS17/1906-2 | 0.150 | 10 | 15 | 0 | 0 | 0.175 | 0.009 | 0.059 | 0.004 |
| 22725 | PS17/1906-2 | 1.805 | 85 | 18 | 3 | 17 | 0.328 | 0.010 | 0.144 | 0.007 |
| 22726 | PS17/1906-2 | 2.005 | 111 | 20 | 1 | 5 | 0.351 | 0.016 | 0.160 | 0.007 |
| 22727 | PS17/1906-2 | 2.105 | 117 | 18 | 1 | 6 | 0.357 | 0.009 | 0.171 | 0.007 |
| 22728 | PS17/1906-2 | 2.205 | 122 | 21 | 1 | 5 | 0.379 | 0.016 | 0.191 | 0.015 |
| 22729 | PS17/1906-2 | 3.290 | 207 | 6 | 1 | 17 | 0.443 | 0.050 | 0.258 | 0.056 |
| [b]22730 | PS17/1906-2 | 3.605 | 225 | 6 | 0 | 0 | 0.343 | 0.014 | 0.160 | 0.023 |
| 22731 | PS17/1906-2 | 5.505 | 398 | 6 | 0 | 0 | 0.517 | 0.018 | 0.331 | 0.026 |

[a] Number of subsamples used to calculate the mean and standard deviation. [b] Stratigraphically reversed sample.

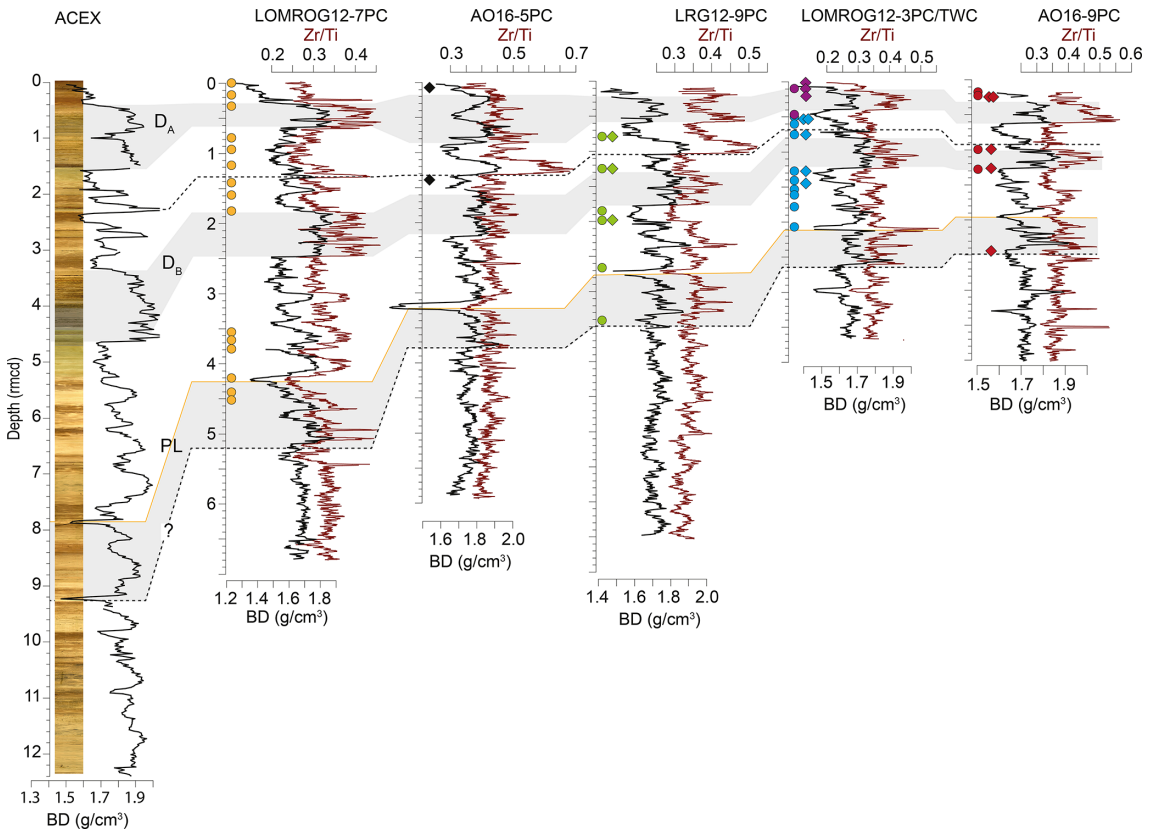


**Figure 2.** Bulk density (BD) (black line) and XRF-scanning Zr/Ti (red line) profiles of sediment cores from the central Arctic Ocean, with correlations among cores and with the ACEX composite section. $D_A$ and $D_B$ are prominent diamict units found in all the cores, while PL is a characteristic fine-grained peach-coloured layer. Locations of *N. pachyderma* (circles) and *C. wuellerstorfi* (triangles) samples analysed in this study are shown for each core.

**Table 3.** Number of rejected subsamples per rejection criterion.

| Species | Total number of subsamples | L-Ser/L-Asp ≥ 0.8 | Non-covarying D/L Asp and D/L Glu | D/L Asp or D/L Glu not within $\pm 2\sigma$ of sample mean |
|---|---|---|---|---|
| *N. pachyderma* | 635 | 81 | 20 | 43 |
| *C. wuellerstorfi* | 374 | 1 | 16 | 20 |

### 3.3 Relationship between D/L values and age/stratigraphic depth

The extent of racemization (D/L values) for Asp and Glu shows a systematic increasing trend with increasing age of samples of both species from the Greenland and Iceland seas, and it follows a simple power function (Fig. 4). A simple power law was used to model the forward rate of racemization in this study, as this is typical for racemization of amino acids in biominerals held under isothermal conditions (e.g. Kaufman, 2006; Clarke and Murray-Wallace, 2006).

The D/L values obtained from sediment cores from the central Arctic Ocean, where age–depth models are less certain, are displayed on the ACEX composite depth scale based on correlations using bulk density profiles (Fig. 5). The extent of racemization follows a simple power function (stratigraphically reversed samples excluded), as also observed in samples from the Nordic Seas, and D/L values generally overlap between correlative samples from multiple cores. This directly supports the accuracy of the lithostratigraphic correlations established among the sites. The D/L values from *N. pachyderma* appear to reach a plateau at ∼ 0.4 for Asp and ∼ 0.2 for Glu (∼ 6 m depth in the ACEX record). Plateauing of D/L Asp values was previously documented in other Arctic Ocean cores as well (Kaufman et al., 2008). It is unclear whether plateauing is present in *C. wuellerstorfi* samples, as only a few samples were analysed in the cor-

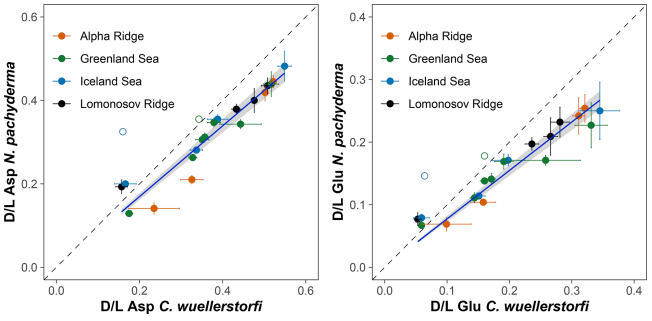


**Figure 3.** Extent of racemization for aspartic acid (Asp) and glutamic acid (Glu) in *N. pachyderma* and *C. wuellerstorfi* from samples from the same stratigraphic depths collected from different regions of the Arctic Ocean. Error bars represent $\pm 1\sigma$ intra-sample variability; solid line is the least-squares regression fit with 95 % confidence interval shown in grey, and the dashed line is the line of equality. Open symbols mark the samples excluded from the regression analysis.

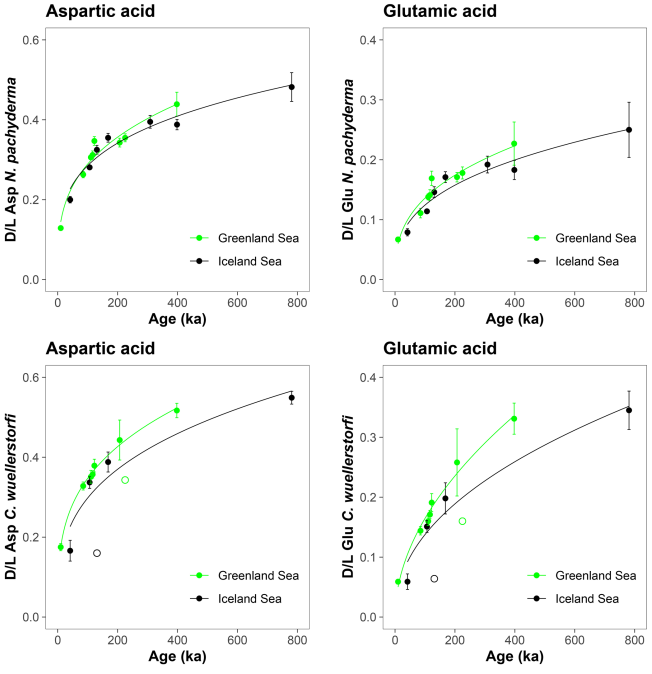


**Figure 4.** Extent of racemization for aspartic acid (Asp) and glutamic acid (Glu) in samples of *N. pachyderma* and *C. wuellerstorfi* from sediment cores PS17/1906-2 (Greenland Sea) and ODP 151/907A (Iceland Sea). Error bars represent $\pm 1\sigma$ intra-sample variability and curves are power functions. Stratigraphically reversed samples are marked with unfilled symbols and were excluded to improve the goodness of fit.

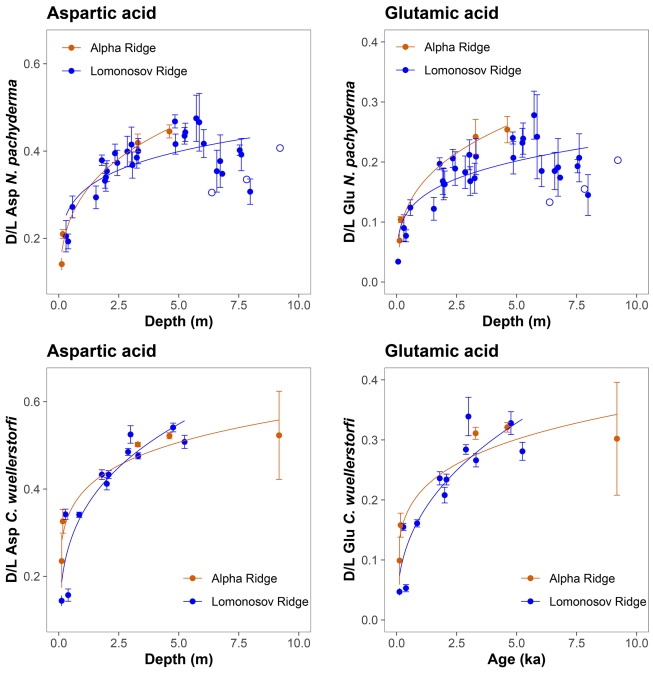


**Figure 5.** Extent of racemization for aspartic acid (Asp) and glutamic acid (Glu) in *N. pachyderma* and *C. wuellerstorfi* from the central Arctic Ocean displayed on the ACEX composite depth. Sediment cores investigated in this study were grouped based on their geographical location (Alpha Ridge – red, Lomonosov Ridge – blue). Error bars are $\pm 1\sigma$ intra-sample variability, curves are power functions, and unfilled symbols mark stratigraphically reversed samples.

responding age range, and the oldest sample has the largest intra-sample variability.

## 4 Discussion

Aspartic acid and glutamic acid racemization analyses of multiple foraminifera taxa obtained from cold bottom water sites across the globe showed that sample ages can be confidently estimated by calibrated age equations, which relate the extent of racemization of the amino acids to independently determined sample age (Kaufman et al., 2013). These globally derived age equations are based on both planktic and benthic foraminifera species with *N. pachyderma* contributing up to ∼21 % of all samples, but *C. wuellerstorfi* is not represented. Ages derived using the global age equations generally agree with independently derived ages at the Yermak Plateau (West et al., 2019) but do not agree with previously published age models from the central Arctic Ocean, beyond about 40 ka. If existing age models in the central Arctic Ocean are correct, the extent of racemization for *N. pachyderma* is higher than expected when compared with other oceans (Kaufman et al., 2008, 2013).

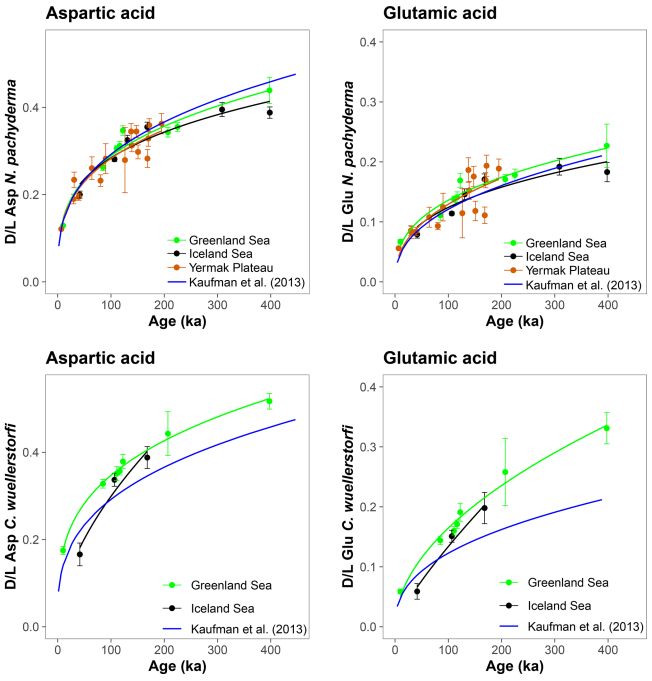


**Figure 6.** Extent of racemization in aspartic acid (Asp) and glutamic acid (Glu) in *Neogloboquadrina pachyderma* and *Cibicidoides wuellerstorfi* from the Greenland and Iceland seas and the Yermak Plateau. Black, green, and red curves are power functions fit to the data. Blue curves are the globally calibrated age equations of Kaufman et al. (2013). Data for the Yermak Plateau are from West et al. (2019). Error bars represent $\pm 1\sigma$ intra-sample variability.

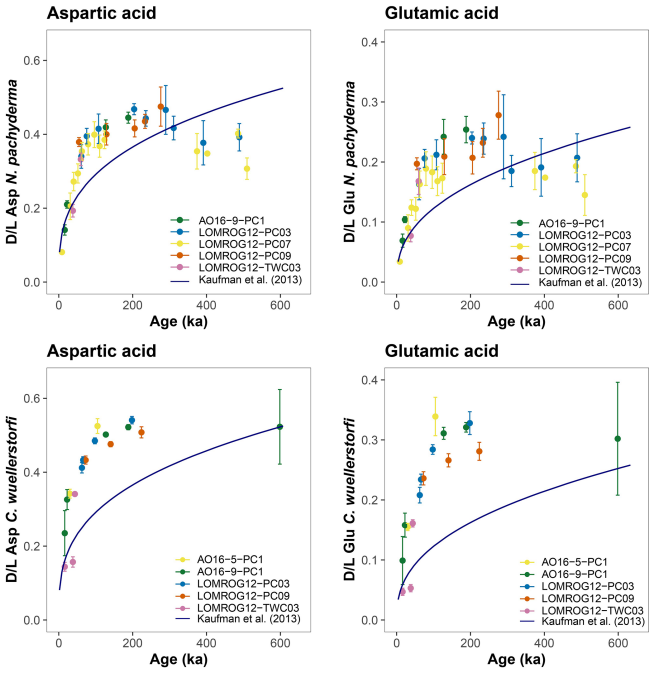


**Figure 7.** Extent of racemization for aspartic acid (Asp) and glutamic acid (Glu) in *N. pachyderma* and *C. wuellerstorfi* from the central Arctic Ocean. The D/L values are displayed against the ACEX age model; D/L values versus age trend defined by the globally calibrated age equations (Kaufman et al., 2013) are shown in blue. Error bars represent $\pm 1\sigma$ intra-sample variability.

The results of AAR presented here show that Asp and Glu racemize in a predictable manner in both *N. pachyderma* and *C. wuellerstorfi* samples from the Nordic Seas (Fig. 4), although the rates differ systematically between the species (Fig. 3). Both D/L Asp and D/L Glu values obtained from *N. pachyderma* samples from the Nordic Seas clearly follow a trend previously observed at the Yermak Plateau (Fig. 6), implying that racemization kinetics are indistinguishable in these areas. These data from independently dated cores from cold water sites provide further support for the integrity of the AAR technique and for the globally calibrated age equations of Kaufman et al. (2013).

The interspecies comparisons show that Asp racemizes approximately 16 % faster in *C. wuellerstorfi* than in *N. pachyderma* (Fig. 3). Differences of similar magnitude were previously observed between *N. pachyderma* and *Pulleniatina obliquiloculata*, in which Asp racemizes 12 %–16 % faster than in *N. pachyderma* (Kaufman et al., 2013). Quantifying the relative differences of the racemization rates between species can facilitate future AAR studies. When a taxon is unavailable at a certain stratigraphic depth, the extent of racemization in one species could be adjusted to that of another based on the difference in the observed rate of racemization. *Cibicidoides wuellerstorfi* was not represented in the globally calibrated age equations and the higher rate of AAR in this species suggests that D/L values should not be used in combination with the equations without adjustment (Fig. 6).

The purportedly higher rates of racemization in *N. pachyderma* from the central Arctic Ocean were argued to be caused by factors other than taxonomic effects (Kaufman et al., 2013). Either racemization generally progresses at a higher rate here due to an unknown reason, or existing age models used to constrain the rate of AAR from the central Arctic Ocean underestimate the true age of deposition. Given the existing age models, higher-than-expected rates of racemization are also observed in this study in both *N. pachyderma* and *C. wuellerstorfi* samples from the central Arctic Ocean (Fig. 7). Differences between ages predicted by the globally calibrated age equation and currently available sample ages based on the ACEX age model are larger for *C. wuellerstorfi*, as expected, since racemization proceeds faster in this taxon than in *N. pachyderma*.

The AAR trends in *C. wuellerstorfi* samples from the Nordic Seas, where age models are better constrained, can also be compared with those in the central Arctic Ocean samples. The racemization of Asp and Glu in *C. wuellerstorfi* samples from both the Greenland and Iceland seas (GIS) follow the same trend (Fig. 4), which can be approximated with

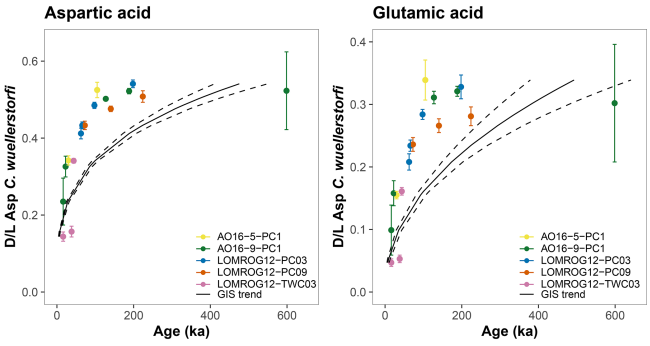


**Figure 8.** Aspartic acid (Asp) and glutamic acid (Glu) racemization versus sample age in *C. wuellerstorfi* from the central Arctic Ocean. Black curves are the age equations determined by samples from the Greenland and Iceland seas (GIS trend); black dashed curves mark 95 % confidence intervals. Error bars represent $\pm 1\sigma$ intra-sample variability.

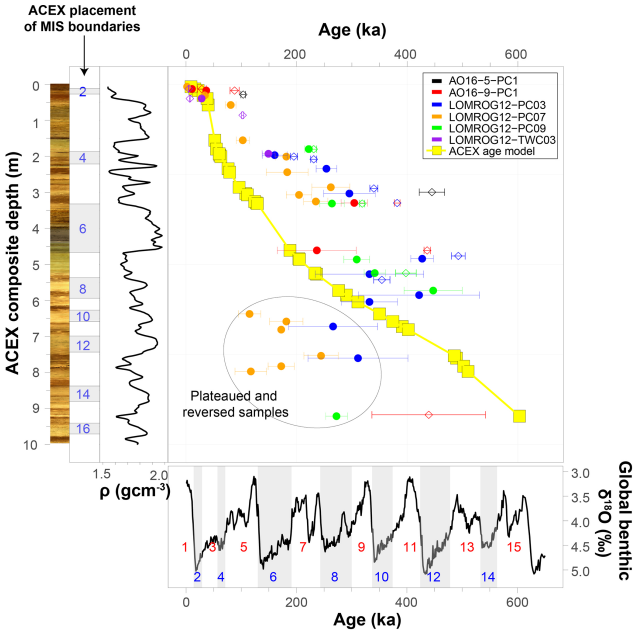


**Figure 9.** Alternative age–depth relationships in sediment cores from the central Arctic Ocean. Circles and diamonds mark ages estimated by globally calibrated rates of racemization of aspartic acid in *N. pachyderma* (Kaufman et al., 2013) and GIS-calibrated rates of racemization of aspartic acid in *C. wuellerstorfi* (this study), respectively. Error bars represent 95 % confidence intervals. The ACEX age model is based on Backman et al. (2008), Frank et al. (2008), and O'Regan et al. (2008). Also shown are the ACEX digital core image, the marine oxygen isotope stage (MIS) boundaries based on the ACEX age model, the bulk density ($\rho$) profile of the ACEX core, and the global benthic $\delta^{18}$O record and corresponding MIS 1–15 based on Lisiecki and Raymo (2005).

regression analysis. Following the removal of stratigraphically reversed samples ($n = 3$) and samples with high analytical uncertainty (coefficient of variation $> 10\,\%$, $n = 5$), simple power functions (Eqs. 1 and 2) fit the D/L Asp and D/L Glu versus age relationship well for the past 400 ka (the period for which these models are robust):

$$t = 3827.6 \cdot (\text{D/L Asp})^{3.395}, \quad (1)$$

$$t = 4979.1 \cdot (\text{D/L Glu})^{2.138}, \quad (2)$$

where $t$ is the age in ka. Applying these equations to D/L values in *C. wuellerstorfi* from the central Arctic Ocean reveals that sample ages are younger than predicted by the model based on the Nordic Sea samples (Fig. 8). The higher-than-expected D/L values observed for *C. wuellerstorfi* from the central Arctic Ocean confirm earlier findings, which argued that higher racemization rates in the central Arctic Ocean are not the result of taxonomic effects (Kaufman et al., 2013).

The discrepancy between the globally (*N. pachyderma*) and GIS (*C. wuellerstorfi*) calibrated AAR ages and the established chronology for central Arctic Ocean sediments are illustrated in Fig. 9 and Table 4. The calibrated AAR ages suggest that intervals previously interpreted as substages in MIS 5 are instead separate interglacial periods extending back to MIS 9. This interpretation would indicate that the diamict unit previously assigned to MIS 6, and representing the onset of a fundamentally different depositional regime in the Arctic characterized by recurrent coarse-grained facies (O'Regan et al., 2010), is likely older than MIS 8 and possibly as old as MIS 12. Exact age determinations are difficult due to a paucity of data from these lower depths and increased downcore scatter in the stacked AAR results (discussed below).

It cannot be excluded that the established chronologies of the central Arctic Ocean sediments underestimate their true ages, but significant shifts (representing multiple glacial cycles) in sediment ages are required. It is important to recognize that this results in a number of fundamental inconsistencies when compared with other geochronological data. For example, recent work (O'Regan et al., 2020) placed the first occurrence of the coccolithophore, *Emiliania huxleyi*, in core LOMROG12-PC03 at $1.39 \pm 0.02$ m b.s.f. in MIS 7 ($\sim 220$ ka). The AAR ages in Eqs. (1) and (2), defined by the trend in *C. wuellerstorfi* samples from the Greenland and Iceland seas, yield estimated ages of $475 \pm 12$ ka (D/L Asp) or $459 \pm 21$ ka (D/L Glu) (MIS 12/13) based on the mean D/L $\pm$ 1SE for a sample from 1.27 m in this core. Similarly, the globally calibrated age equation (Kaufman et al., 2013) returns an MIS 12 age of $427 \pm 20$ ka for *N. pachyderma* samples from 1.29 m in LOMROG12-PC03. These ages are substantially older than the evolutionary occurrence of *E. huxleyi* during MIS 8 (Thierstein et al., 1977; Anthonissen and Ogg, 2012). Furthermore, *E. huxleyi* is abundant in the 0.58–0.82 m b.s.f. core interval of LOMROG12-PC03, which was assigned an MIS 5 age (O'Regan et al., 2020). In contrast, the AAR trend from the Greenland and Iceland seas assigns ages of $189 \pm 6$ to $328 \pm 7$ ka (MIS 6–9) for the 0.52–0.74 m

**Table 4.** Age estimates for selected stratigraphic intervals in core LOMROG12-PC03 based on the ACEX age model and occurrences of *E. huxleyi* and AAR geochronology.

| Stratigraphic depth (m) | ACEX equivalent depth (m) | Marine isotope stage (MIS) correlation | | |
|---|---|---|---|---|
| | | ACEX age model (Backman et al., 2008; O'Regan et al., 2008) and *E. huxleyi* occurrences (O'Regan et al., 2020) | AAR geochronology – aspartic acid in *N. pachyderma* (Kaufman et al., 2013) | AAR geochronology – aspartic acid in *C. wuellerstorfi* (this study) |
| 0.52–0.74 | 1.96–3.35 | MIS 5 | MIS 6–9 | MIS 6–9 |
| 1.27–1.39 | 4.62–5.44 | MIS 7 | MIS 9–12 | MIS 9–12 |

core depths (Table 4). This could only be reconciled with the existence of *E. huxleyi* in this interval if it had entered the Arctic shortly after its first evolutionary occurrence. However, the MIS 6–9 age is not consistent with results from optically stimulated luminescence dating in stratigraphically coeval sediments from another core on the Lomonosov Ridge, which support the MIS 5 age assignment (Jakobsson et al., 2003).

On the other hand, sedimentation rates estimated using the AAR global and GIS calibration equations are consistent with radiocarbon-derived estimates over the past 40 ka, but beyond this point remain intermediate between the proposed age model for the ACEX record (O'Regan et al., 2008) and those recently inferred from $^{230}$Th and $^{231}$Pa extinction ages in sedimentary sequences from this region of the Lomonosov Ridge (Hillaire-Marcel et al., 2017; Purcell et al., 2022). Additional work is required to understand the origin and resolve the differences between these geochronological approaches. However, a critical observation is that even the older estimated ages from the global and GIS calibration equations remain considerably younger than the long-overturned palaeomagnetic-derived age model that would place the Bruhnes–Matuyama boundary ($\sim$ 780 ka) at approximately 5 m depth in the ACEX record (O'Regan et al., 2008) (Fig. 9).

An alternative to central Arctic Ocean age models underestimating the true age of sediments is that the rate of AAR in foraminifera from the central Arctic Ocean is faster than in the eastern Arctic Ocean (West et al., 2019), the Nordic Seas (this study), and other globally distributed cold water sites (Kaufman et al., 2013). A fundamental premise of this study is that the investigated central Arctic Ocean sites have experienced similar temperature histories to those other cold water sites. Modern bottom water temperatures near the coring sites are very similar (Table 1), but they may have differed in the past. Cronin et al. (2012) showed that the central Arctic basin waters, at $\sim$ 1000–2500 m depth interval, were 1–2 °C warmer during the past 50–11 ka than today. While this might account for part of the apparently higher rate of AAR in the central Arctic Ocean, West et al. (2019) showed that more substantial differences ($\sim >$ 4 °C) in effective diagenetic temperatures would be required to achieve the differences observed between D/L values of equivalent age samples from sediment cores from the central Arctic Ocean and those from the Nordic Seas. Available heat flow data (Shephard et al., 2018) show that geothermal flux is not unusually high in the central Arctic Ocean when compared to the Yermak Plateau, and thus cannot explain the apparently higher rates of racemization. Therefore, while offsets in D/L values in stratigraphically coeval sections of different central Arctic Ocean cores in this study might, in part, be attributed to differences in bottom water temperatures, it is unlikely that such differences are able to explain the overall higher inferred rates of racemization compared to other global sites.

The D/L values in many samples of *N. pachyderma* from the central Arctic Ocean cores exhibit a distinct plateauing below the $\sim$ 5.5–6 m composite ACEX depth (Figs. 5 and 9). Some of these samples are stratigraphically reversed (i.e. their D/L values are lower than of those from shallower depths). Such plateauing of D/L values was previously observed in cores from other areas of the Arctic Ocean (Kaufman et al., 2008), but its cause remains unclear. While sediment mass movements, glacial erosion, and subsequent redeposition are known to occur across the Arctic Ocean (e.g. Jakobsson and O'Regan, 2016; Boggild et al., 2020; Pérez et al., 2020; Schlager et al., 2021), this explanation would require that almost all of the material above 5.5–6 m composite depth was reworked similarly across multiple cores, which seems highly unlikely.

Local differences in sedimentation rates might also account for some of the observed scatter in AAR results. For example, there are pronounced regional differences in the thickness of correlative units in the studied cores (Fig. 2), implying highly variable sedimentation rates between the sites. In cores with lower sedimentation rates, the influence of bioturbation could conceivably introduce significant scatter though mixing of individuals of different ages.

Overall, sedimentation rates in the central Arctic Ocean are much lower in marginal areas closer to the shelves (Backman et al., 2004) and can be greatly reduced during glacials in some regions of the Arctic Ocean (Jakobsson et al., 2014). Conversely, thick diamict units suggest rapid influxes of ice-rafted material during some glacials or glacial terminations. These punctuated episodes of sedimentation can not only introduce hiatuses but also impact the length of time biocarbonates are exposed to microbial activity on the seafloor (Se-

jrup and Haugen, 1994), which in turn can speed up or slow down organic diagenetic processes that influence the rate of AAR. For example, where sedimentation rates are low, greater microbial activity could increase organic diagenesis and lead to higher apparent rates of AAR. On the other hand, continuous turnover and reworking of microbial necromass within the foraminifera test could instead lower the apparent rate of racemization via regeneration of L-amino acids, and alter the apparent AAR rates, as has been documented for bulk organic matter in marine sediments (Braun et al., 2017). The composition of the microbial community may also have an impact. Kubota et al. (2016) isolated Alphaproteobacteria from deep-sea sediments from the Sagami Bay (Japan), which exclusively utilized D-amino acids as a carbon and nitrogen source. If such microbes were also present within foraminifera tests of the central Arctic Ocean, they could potentially alter the progress of racemization. Apparent plateauing of D/L values (e.g. Figs. 5, 7, 9) could be associated with these processes but would require a distinctively different microbial sedimentary environment in the central Arctic Ocean than elsewhere (such as the Yermak Plateau or Norwegian–Greenland Sea, where the global age equation appears applicable). This is not inconceivable, as recently Yu et al. (2020) suggested that different marine environments could be characterized by distinct bacterial groups that utilize D-amino acids.

In the future, pretreating the foraminifera tests with bleach to isolate the intra-crystalline fraction, which approximates a closed system during diagenesis (Penkman et al., 2008; Wheeler et al., 2021), could minimize the influence of bacterial activity on racemization rates. However, recent work (Millman et al., 2022) showed that bleaching does not necessarily improve the quality of AAR results in foraminifera, thus the current study used the standard weak oxidative pretreatment. Future work should investigate how bleaching impacts AAR results from central Arctic Ocean cores.

If the rate of AAR in foraminifera is indeed higher in the central Arctic Ocean, its exact cause remains unknown. The data reported in this study confirm that it is not caused by taxonomic effects. It is observed not only in the planktic *N. pachyderma* but also in the benthic species *C. wuellerstorfi*. We have highlighted the discrepancies that arise in central Arctic Ocean age models if the global (*N. pachyderma*) and GIS (*C. wuellerstorfi*) AAR age equations are applied. This alternate geochronological interpretation should be considered in future attempts to reconcile the currently disparate results from different dating techniques applied to Arctic Ocean sediments.

## 5 Conclusions

Aspartic acid and glutamic acid racemize faster in *C. wuellerstorfi* than in *N. pachyderma*, and the extent of racemization for these amino acids increases progressively with sample age in both species from multiple sediment cores. Their trends conform to a simple power function.

*C. wuellerstorfi* samples are characterized by lower intra-sample variability than those of *N. pachyderma*, and this, coupled with a reduced subsample rejection rate and faster sample processing offered by its larger tests make it an appealing target of future AAR studies.

Ages of *N. pachyderma* samples from the Greenland and Iceland seas agree with ages predicted by globally calibrated age equations for aspartic acid and glutamic acids (Kaufman et al., 2013) and confirm their applicability in these polar regions.

The rate of racemization for *C. wuellerstorfi* was calibrated for the past 400 ka using samples from the Greenland and Iceland seas. Applying this calibration to the *C. wuellerstorfi* samples from the central Arctic Ocean indicates that they are older than their currently accepted ages. This confirms that higher-than-expected D/L values in *N. pachyderma* from the central Arctic Ocean are not the result of taxonomic effects.

We cannot find a clear reason why calibrated age equations that work globally in the eastern Arctic Ocean and in the Nordic Seas cannot be applied in the central Arctic Ocean. As such, the older ages predicted by these equations for central Arctic Ocean sediments remain a viable option when comparing and assessing results from different approaches to dating Arctic marine sediments.

Regardless of the age equation applied, substantial scatter remains in the AAR age estimates for stratigraphically coeval intervals in central Arctic Ocean cores. This is likely to reflect a combination of enhanced mixing in low sedimentation rate environments, differences in effective diagenetic burial temperatures, and potentially the poorly defined role of microbial activity.

**Data availability.** The results of amino acid analyses of all 1009 subsamples included in this study are archived at the World Data Service for Paleoclimatology (https://doi.org/10.25921/bx56-4d69, West et al., 2023).

**Supplement.** The supplement related to this article is available online at: https://doi.org/10.5194/gchron-5-285-2023-supplement.

**Author contributions.** GW: conceptualization, formal analysis, funding acquisition, investigation, visualization, and writing – original draft preparation, review, and editing. DSK: conceptualization, data curation, formal analysis, funding acquisition, resources, and writing – review and editing. MJ: conceptualization, resources, and writing – review and editing. MO'R: conceptualization, funding acquisition, resources, project administration, and writing – review and editing.

**Competing interests.** The contact author has declared that none of the authors has any competing interests.



**Acknowledgements.** We thank all expedition crew members and scientific parties who facilitated data collection. We further thank Jutta Wollenburg, Jens Matthiessen, and the IODP Bremen Core Repository for providing samples from the Greenland and Iceland seas, and Jordon Bright, Joshua Smith, and Katherine Whitacre for laboratory assistance.

**Financial support.** Funding for this research was provided by the Swedish Research Council (grant no. DNR-2016-05092), the Bolin Centre for Climate Research (Ref. RA6_21_05), and the US National Science Foundation (grant no. 1855381).

**Review statement.** This paper was edited by Georgina King and reviewed by Colin V. Murray-Wallace and two anonymous referees.

## References

Alexanderson, H., Backman, J., Cronin, T. M., Funder, S., Ingólfsson, Ó., Jakobsson, M., Landvik, J. Y., Löwemark, L., Mangerud, J., März, C., Möller, P., O'Regan, M., and Spielhagen, R. F.: An Arctic perspective on dating Mid-Late Pleistocene environmental history, Quaternary Sci. Rev., 92, 9–31, https://doi.org/10.1016/j.quascirev.2013.09.023, 2014.

Anthonissen, D. E. and Ogg, J. G.: Cenozoic and Cretaceous Biochronology of Planktonic Foraminifera and Calcareous Nannofossils, in: The Geologic Time Scale, edited by: Gradstein, F. M., Ogg, J. G., Schmitz, M., and Ogg, G., Elsevier, 1083–1127, https://doi.org/10.1016/B978-0-444-59425-9.15003-6, 2012.

Backman, J., Jakobsson, M., Lvlie, R., Polyak, L., and Febo, L. A.: Is the central Arctic Ocean a sediment starved basin?, Quaternary Sci. Rev., 20, 1435–1454, https://doi.org/10.1016/j.quascirev.2003.12.005, 2004.

Backman, J., Jakobsson, M., Frank, M., Sangiorgi, F., Brinkhuis, H., Stickley, C., O'Regan, M., Løvlie, R., Pälike, H., Spofforth, D., Gattacecca, J., Moran, K., King, J., and Heil, C.: Age model and core-seismic integration for the Cenozoic Arctic Coring Expedition sediments from the Lomonosov Ridge, Paleoceanography, 23, PA1S01, https://doi.org/10.1029/2007PA001476, 2008.

Bauch, H. A.: Sedimentation rate of sediment core PS1906-2, PANGAEA, https://doi.org/10.1594/PANGAEA.82396, 2002.

Bauch, H. A.: Interglacial climates and the Atlantic meridional overturning circulation: is there an Arctic controversy?, Quaternary Sci. Rev., 63, 1–22, https://doi.org/10.1016/j.quascirev.2012.11.023, 2013.

Boggild, K., Mosher, D. C., Travaglini, P., Gebhardt, C., and Mayer, L.: Mass wasting on Alpha Ridge in the Arctic Ocean: new insights from multibeam bathymetry and sub-bottom profiler data, Geol. Soc. Lond. Spec. Publ., 500, 323–340, https://doi.org/10.1144/SP500-2019-196, 2020.

Braun, S., Mhatre, S. S., Jaussi, M., Røy, H., Kjeldsen, K. U., Pearce, C., Seidenkrantz, M.-S., Jørgensen, B. B., and Lomstein, B. Aa.: Microbial turnover times in the deep seabed studied by amino acid racemization modelling, Sci. Rep., 7, 5680, https://doi.org/10.1038/s41598-017-05972-z, 2017.

Burkett, A. M., Rathburn, A. E., Elena Pérez, M., Levin, L. A., and Martin, J. B.: Colonization of over a thousand *Cibicidoides wuellerstorfi* (foraminifera: Schwager, 1866) on artificial substrates in seep and adjacent off-seep locations in dysoxic, deep-sea environments, Deep-Sea Res. Pt. I, 117, 39–50, https://doi.org/10.1016/j.dsr.2016.08.011, 2016.

Clarke, S. J. and Murray-Wallace, C. V.: Mathematical expressions used in amino acid racemisation geochronology – a review, Quat. Geochronol., 1, 261–278, https://doi.org/10.1016/j.quageo.2006.12.002, 2006.

Cronin, T. M., Dwyer, G. S., Farmer, J., Bauch, H. A., Spielhagen, R. F., Jakobsson, M., Nilsson, J., Briggs, W. M., and Stepanova, A.: Deep Arctic Ocean warming during the last glacial cycle, Nat. Geosci., 5, 631–634, https://doi.org/10.1038/ngeo1557, 2012.

Cronin, T. M., Keller, K. J., Farmer, J. R., Schaller, M. F., O'Regan, M., Poirier, R., Coxall, H., Dwyer, G. S., Bauch, H., Kindstedt, I. G., Jakobsson, M., Marzen, R., and Santin, E.: Interglacial paleoclimate in the Arctic, Paleoceanography, 34, 1959–1979, https://doi.org/10.1029/2019PA003708, 2019.

Darling, K. F., Wade, C. M., Siccha, M., Trommer, G., Schulz, H., Abdolalipour, S., and Kurasawa, A.: Genetic diversity and ecology of the planktonic foraminifers *Globigerina bulloides*, *Turborotalita quinqueloba* and *Neogloboquadrina pachyderma* off the Oman margin during the late SW Monsoon, Mar. Micropaleontol., 137, 64–77, https://doi.org/10.1016/j.marmicro.2017.10.006, 2017.

Frank, M., Backman, J., Jakobsson, M., Moran, K., O'Regan, M., King, J., Haley, B. A., Kubik, P. W., and Garbe-Schönberg, D.: Beryllium isotopes in central Arctic Ocean sediments over the past 12.3 million years: Stratigraphic and paleoclimatic implications, Paleoceanography, 23, PA1S02, https://doi.org/10.1029/2007PA001478, 2008.

Hanslik, D., Löwemark, L., and Jakobsson, M.: Biogenic and detrital-rich intervals in central Arctic Ocean cores identified using X-ray fluorescence scanning, Polar Res., 32, 18386, https://doi.org/10.3402/polar.v32i0.18386, 2013.

Haugen, J.-E., Sejrup, H. P., and Vogt, N. B.: Chemotaxonomy of Quaternary benthic foraminifera using amino acids, J. Foramin. Res., 19, 38–51, https://doi.org/10.2113/gsjfr.19.1.38, 1989.

Hillaire-Marcel, C., Ghaleb, B., de Vernal, A., Maccali, J., Cuny, K., Jacobel, A., Le Duc, C., and McManus, J.: A new chronology of late quaternary sequences from the central Arctic Ocean based on "extinction ages" of their excesses in $^{231}$Pa and $^{230}$Th, Geochem. Geophy. Geosy., 18, 4573–4585, https://doi.org/10.1002/2017GC007050, 2017.

Jakobsson, M. and O'Regan, M.: Deep iceberg ploughmarks in the central Arctic Ocean, Geol. Soc. Lond. Mem., 46, 287–288, https://doi.org/10.1144/M46.14, 2016.

Jakobsson, M., Løvlie, R., Arnold, E. M., Backman, J., Polyak, L., Knutsen, J. O., and Musatov, E.: Pleistocene stratigraphy and paleoenvironmental variation from Lomonosov Ridge sed-

iments, central Arctic Ocean. Global Planet. Change, 31, 1–22, https://doi.org/10.1016/S0921-8181(01)00110-2, 2001.

Jakobsson, M., Backman, J., Murray, A., and Løvlie, R.: Optically stimulated luminescence dating supports central Arctic Ocean cm-scale sedimentation rates, Geochem. Geophy. Geosy., 4, 1016, https://doi.org/10.1029/2002GC000423, 2003.

Jakobsson, M., Andreassen, K., Bjarnadóttir, L. R., Dove, D., Dowdeswell, J. A., England, J. H., Funder, S., Hogan, K., Ingólfsson, Ó., Jennings, A., Krog Larsen, N., Kirchner, N., Landvik, J. Y., Mayer, L., Mikkelsen, N., Möller, P., Niessen, F., Nilsson, J., O'Regan, M., Polyak, L., Nørgaard-Pedersen, N., and Stein, R.: Arctic Ocean glacial history, Quaternary Sci. Rev., 92, 40–67, https://doi.org/10.1016/j.quascirev.2013.07.033, 2014.

Jakobsson, M., Mayer, L. A., Bringensparr, C., Castro, C. F., Mohammad, R., Johnson, P., Ketter, T., Accettella, D., Amblas, D., An, L., Arndt, J. E., Canals, M., Casamor, J. L., Chauché, N., Coakley, B., Danielson, S., Demarte, M., Dickson, M.-L., Dorschel, B., Dowdeswell, J. A., Dreutter, S., Fremand, A. C., Gallant, D., Hall, J. K., Hehemann, L., Hodnesdal, H., Hong, J., Ivaldi, R., Kane, E., Klaucke, I., Krawczyk, D. W., Kristoffersen, Y., Kuipers, B. R., Millan, R., Masetti, G., Morlighem, M., Noormets, R., Prescott, M. M., Rebesco, M., Rignot, E., Semiletov, I., Tate, A. J., Travaglini, P., Velicogna, I., Weatherall, P., Weinrebe, W., Willis, J. K., Wood, M., Zarayskaya, Y., Zhang, T., Zimmermann, M., and Zinglersen, K. B.: The International Bathymetric Chart of the Arctic Ocean Version 4.0, Sci. Data, 7, 176, https://doi.org/10.1038/s41597-020-0520-9, 2020.

Jansen, E., Fronval, T., Rack, F., and Channell, J. E. T.: IRD tuned age model of ODP Site 151-907, PANGAEA, https://doi.org/10.1594/PANGAEA.848080, 2000a.

Jansen, E., Fronval, T., Rack, F., and Channell, J. E. T.: Pliocene-Pleistocene ice rafting history and cyclicity in the Nordic Seas during the last 3.5 Myr, Paleoceanography, 15, 709–721, https://doi.org/10.1029/1999PA000435, 2000b.

Kaufman, D., Cooper, K., Behl, R., Billups, K., Bright, J., Gardner, K., Hearty, P., Jakobsson, M., Mendes, I., O'Leary, M., Polyak, L., Rasmussen, T., Rosa, F., and Schmidt, M.: Amino acid racemization in mono-specific foraminifera from Quaternary deep-sea sediments, Quat. Geochronol., 16, 50–61, https://doi.org/10.1016/j.quageo.2012.07.006, 2013.

Kaufman, D. S.: Temperature sensitivity of aspartic and glutamic acid racemization in the foraminifera *Pulleniatina*, Quat. Geochronol., 1, 188–207, https://doi.org/10.1016/j.quageo.2006.06.008, 2006.

Kaufman, D. S. and Manley, W. F.: A new procedure for determining DL amino acid ratios in fossils using reverse phase liquid chromatography, Quaternary Sci. Rev., 17, 987–1000, https://doi.org/10.1016/S0277-3791(97)00086-3, 1998.

Kaufman, D. S., Polyak, L., Adler, R., Channell, J. E. T., and Xuan, C.: Dating late Quaternary planktonic foraminifer *Neogloboquadrina pachyderma* from the Arctic Ocean using amino acid racemization, Paleoceanography, 23, PA3224, https://doi.org/10.1029/2008PA001618, 2008.

King, K. and Neville, C.: Isoleucine epimerization for dating marine sediments: Importance of analyzing monospecific foraminiferal samples, Science, 195, 1333–1335, https://doi.org/10.1126/science.195.4284.1333, 1977.

Kosnik, M. A. and Kaufman, D. S.: Identifying outliers and assessing the accuracy of amino acid racemization measurements for geochronology: II. Data screening, Quat. Geochronol., 3, 328–341, https://doi.org/10.1016/j.quageo.2008.04.001, 2008.

Kubota, T., Kobayashi, T., Nunoura, T., Maruyama, F., and Deguchi, S. Enantioselective utilization of D-amino acids by deep-sea microorganisms, Front. Microbiol., 7, 511, https://doi.org/10.3389/fmicb.2016.00511, 2016.

Lisiecki, L. E. and Raymo, M. E.: A Pliocene-Pleistocene stack of 57 globally distributed benthic $\delta^{18}$O records, Paleoceanography, 20, PA1003, https://doi.org/10.1029/2004PA001071, 2005.

Locarnini, R. A., Mishonov, A. V., Baranova, O. K., Boyer, T. P., Zweng, M. M., Garcia, H. E., Reagan, J. R., Seidov, D., Weathers, K. W., Paver, C. R., and Smolyar, I. V.: World Ocean Atlas 2018, Volume 1: Temperature, Mishonov, A. (Technical Editor), NOAA Atlas NESDIS 81, 52 pp., 2018.

Millman E., Wheeler L., Billups K., Kaufman D., and Penkman K. E.: Testing the effect of oxidizing pre-treatments on amino acids in benthic and planktic foraminifera tests, Quat. Geochronol., 73, 101401, https://doi.org/10.1016/j.quageo.2022.101401, 2022.

O'Regan, M., King, J., Backman, J., Jakobsson, M., Pälike, H., Moran, K., Heil, C., Sakamoto, T., Cronin, T. M., and Jordan, R. W.: Constraints on the Pleistocene chronology of sediments from the Lomonosov Ridge, Paleoceanography, 23, PA1S19, https://doi.org/10.1029/2007PA001551, 2008.

O'Regan, M., John, K. S., Moran, K., Backman, J., King, J., Haley, B. A., Jakobsson, M., Frank, M., and Röhl, U.: Plio-Pleistocene trends in ice rafted debris on the Lomonosov Ridge, Quaternary Int., 219, 168–176, https://doi.org/10.1016/j.quaint.2009.08.010, 2010.

O'Regan, M., Coxall, H. K., Cronin, T. M., Gyllencreutz, R., Jakobsson, M., Kaboth, S., Löwemark, L., Wiers, S., and West, G.: Stratigraphic occurrences of sub-polar planktic foraminifera in Pleistocene sediments on the Lomonosov Ridge, Arctic Ocean, Front. Earth Sci., 7, 71, https://doi.org/10.3389/feart.2019.00071, 2019.

O'Regan, M., Backman, J., Fornaciari, E., Jakobsson, M., and West, G.: Calcareous nannofossils anchor chronologies for Arctic Ocean sediments back to 500 ka, Geology, 48, 1115–1119, https://doi.org/10.1130/G47479.1, 2020.

Penkman, K. E., Kaufman, D. S., Maddy, D., and Collins, M. J.: Closed-system behaviour of the intra-crystalline fraction of amino acids in mollusc shells, Quat. Geochronol., 3, 2–25, https://doi.org/10.1016/j.quageo.2007.07.001, 2008.

Pérez, L. F., Jakobsson, M., Funck, T., Andresen, K. J., Nielsen, T., O'Regan, M., and Mørk, F.: Late Quaternary sedimentary processes in the central Arctic Ocean inferred from geophysical mapping, Geomorphology, 369, 107309, https://doi.org/10.1016/j.geomorph.2020.107309, 2020.

Purcell, K., Hillaire-Marcel, C., de Vernal, A., Ghaleb, B., and Stein, R.: Potential and limitation of $^{230}$Th-excess as a chronostratigraphic tool for late Quaternary Arctic Ocean sediment studies: An example from the southern Lomonosov Ridge, Mar. Geol., 448, 106802, https://doi.org/10.1016/j.margeo.2022.106802, 2022.

Raitzsch, M., Rollion-Bard, C., Horn, I., Steinhoefel, G., Benthien, A., Richter, K.-U., Buisson, M., Louvat, P., and Bijma, J.: Technical note: Single-shell $\delta^{11}$B analysis of Cibicidoides wuellerstorfi using femtosecond laser ablation MC-ICPMS and secondary ion mass spectrometry, Biogeosciences, 17, 5365–5375, https://doi.org/10.5194/bg-17-5365-2020, 2020.

Rasmussen, T. L. and Thomsen, E.: Ecology of deep-sea benthic foraminifera in the North Atlantic during the last glaciation: Food or temperature control, Palaeogeogr. Palaeocl., 472, 15–32, https://doi.org/10.1016/j.palaeo.2017.02.012, 2017.

Schlager, U., Jokat, W., Weigelt, E., and Gebhardt, C.: Submarine landslides along the Siberian termination of the Lomonosov Ridge, Arctic Ocean, Geomorphology, 382, 107679, https://doi.org/10.1016/j.geomorph.2021.107679, 2021.

Sejrup, H. P. and Haugen, J.-E.: Foraminiferal amino acid stratigraphy of the Nordic Seas: geological data and pyrolysis experiments, Deep-Sea Res. Pt. A, 39, S603–S623, https://doi.org/10.1016/S0198-0149(06)80022-1, 1992.

Sejrup, H. P. and Haugen, J.-E.: Amino acid diagenesis in the marine bivalve *Arctica islandica* Linné from northwest European sites: Only time and temperature?, J. Quaternary Sci., 9, 301–309, https://doi.org/10.1002/jqs.3390090402, 1994.

Sejrup, H. P., Miller, G. H., Brigham-Grette, J., Løvlie, R., and Hopkins, D.: Amino acid epimerization implies rapid sedimentation rates in Arctic Ocean cores, Nature, 310, 772–775, https://doi.org/10.1038/310772a0, 1984.

Shackleton, N. J., Sánchez-Goñi, M. F., Pailler, D., and Lancelot, Y.: Marine Isotope Substage 5e and the Eemian Interglacial, Glob. Planet. Change, 36, 151–155, https://doi.org/10.1016/S0921-8181(02)00181-9, 2003.

Shephard, G. E., Wiers, S., Bazhenova, E., Pérez, L. F., Mejía, L. M., Johansson, C., Jakobsson, M., and O'Regan, M.: A North Pole thermal anomaly? Evidence from new and existing heat flow measurements from the central Arctic Ocean, J. Geodyn., 118, 166–181, https://doi.org/10.1016/j.jog.2018.01.017, 2018.

Spielhagen, R. F., Baumann, K. H., Erlenkeuser, H., Nowaczyk, N. R., Nørgaard-Pedersen, N., Vogt, C., and Weiel, D.: Arctic Ocean deep-sea record of northern Eurasian ice sheet history, Quaternary Sci. Rev., 23, 1455–1483, https://doi.org/10.1016/j.quascirev.2003.12.015, 2004.

Thierstein, H. R., Geitzenauer, K. R., Molfino, B., and Shackleton, N. J.: Global synchroneity of late Quaternary coccolith datum levels validation by oxygen isotopes, Geology, 5, 400, https://doi.org/10.1130/0091-7613(1977)5<400:GSOLQC>2.0.CO;2, 1977.

West, G., Kaufman, D. S., Muschitiello, F., Forwick, M., Matthiessen, J., Wollenburg, J., and O'Regan, M.: Amino acid racemization in Quaternary foraminifera from the Yermak Plateau, Arctic Ocean, Geochronology, 1, 53–67, https://doi.org/10.5194/gchron-1-53-2019, 2019.

West, G., Kaufman, D. S., Jakobsson, M., and O'Regan, M.: Quaternary Arctic Ocean Foraminifer Amino Acid Racemization Data, NCEI [data set], https://doi.org/10.25921/bx56-4d69, 2023.

Wheeler L. J., Penkman K. E., Sejrup H. P.: Assessing the intracrystalline approach to amino acid geochronology of Neogloboquadrina pachyderma (sinistral), Quat. Geochronol., 61, 101131, https://doi.org/10.1016/j.quageo.2020.101131, 2021.

Wollenburg, J. E., Raitzsch, M., and Tiedemann, R.: Novel high-pressure culture experiments on deep-sea benthic foraminifera – Evidence for methane seepage-related $\delta^{13}C$ of *Cibicides wuellerstorfi*, Mar. Micropaleontol., 117, 47–64, https://doi.org/10.1016/j.marmicro.2015.04.003, 2015.

Yu, J. and Elderfield, H.: Mg/Ca in the benthic foraminifera *Cibicidoides wuellerstorfi* and *Cibicidoides mundulus*: Temperature versus carbonate ion saturation, Earth Planet. Sc. Lett., 276, 129–139, https://doi.org/10.1016/j.epsl.2008.09.015, 2008.

Yu, Y., Yang, J., Zheng, L.-Y., Sheng, Q., Li, C.-Y., Wang, M., Zhang, X.-Y., McMinn, A., Zhang, Y.-Z., Song, X.-Y., and Chen, X.-L.: Diversity of D-amino acid utilizing bacteria from Kongsfjorden, Arctic and the metabolic pathways for seven D-amino acids, Front. Microbiol., 10, 2983, https://doi.org/10.3389/fmicb.2019.02983, 2020.